

Fig. 1 Two-dimensional model configuration

Dimensional Analysis

The problem under study is completely determined once (i) the geometry, (ii) the fluid constants, (iii) the external excitation, and (iv) the equations that must be satisfied, are defined. In order to reduce the number of parameters which govern the problem, the dimensionless problem is first to be studied. The problem statement is given in Fig. 1. The two-dimensional rigid container has a depth D and a width W , the dimensions of the submerged blocks are defined in Fig. 1. The fluid is assumed Newtonian, hence, only density, ρ , and viscosity, μ , are needed. The body forces are those due to gravity (only the vertical component is non zero) and imposed vibration (only the horizontal component is non zero). The latter is a prescribed sinusoidal motion, thus, the accelerations in the horizontal and vertical directions are

$$\begin{cases} g_1^* = Ag \sin(\omega^* t^*) \\ g_2^* = -g \end{cases} \quad (1)$$

where g , ω^* , and t^* are the acceleration of gravity, circular frequency, and time, respectively, and A is an arbitrary dimensionless constant governing the amplitude of the excitation. In this section super-star (*) stands for dimensioned variables, lower subscripts denote the components of a tensor, and repeated indices imply summation over the number of spatial dimensions. The continuity and equilibrium equations which must be satisfied, under an ALE formulation, Huerta and Liu (1988), are written as

$$\frac{\partial v_i^*}{\partial x_i^*} = 0 \quad (2a)$$

$$\rho \frac{\partial v_i^*}{\partial t^*} + \rho c_j^* \frac{\partial v_i^*}{\partial x_j^*} = - \frac{\partial P^*}{\partial x_i^*} + \mu \frac{\partial}{\partial x_j^*} \left(\frac{\partial v_i^*}{\partial x_j^*} + \frac{\partial v_j^*}{\partial x_i^*} \right) + \rho g_i^* \quad (2b)$$

where \mathbf{v}^* is the material velocity, \mathbf{x}^* are the spatial coordinates, P^* is the pressure, and \mathbf{c}^* is the convective velocity which is defined in equations (8).

Once the problem definition is completed, the governing characteristic dimensions are chosen: length D , velocity \sqrt{gD} , acceleration g , pressure $\rho g D$, and time $\sqrt{\frac{D}{g}}$. All the

other characteristic dimensions are automatically deduced from these; for instance, the characteristic viscosity and density are, respectively, $\rho \sqrt{g D D}$ and ρ . The problem is rewritten in terms of dimensionless variables:

$$\begin{aligned} v_i &= \frac{v_i^*}{\sqrt{gD}} & x_i &= \frac{x_i^*}{D} \\ i &= 1, \dots, \text{NSD} & t &= \frac{t^*}{\sqrt{\frac{D}{g}}} \\ g_i &= \frac{g_i^*}{g} & P_i &= \frac{P_i^*}{\rho g D} \end{aligned} \quad (3)$$

After substitution of equations (3) into equations (2), the following dimensionless equations are obtained:

$$\frac{\partial v_i}{\partial x_i} = 0 \quad (4a)$$

$$\frac{\partial v_i}{\partial t} + c_j \frac{\partial v_i}{\partial x_j} = - \frac{\partial P}{\partial x_i} + \frac{1}{\text{Re}} \frac{\partial}{\partial x_j} \left(\frac{\partial v_i}{\partial x_j} + \frac{\partial v_j}{\partial x_i} \right) + g_i \quad (4b)$$

where Re is the Reynolds number

$$\text{Re} = \frac{\sqrt{g D D}}{\frac{\mu}{\rho}} \quad (5)$$

The dimensionless external excitation is also obtained when the scaling definitions, equations (3), are substituted into equation (1); namely,

$$\begin{cases} g_1 = \frac{g_1^*}{g} = A \sin(\omega t) \\ g_2 = \frac{g_2^*}{g} = -1 \end{cases} \quad (6)$$

where t is the dimensionless time defined in equations (3), and the dimensionless circular frequency ω is

$$\omega = \omega^* \sqrt{\frac{D}{g}} = 2\pi f \sqrt{\frac{D}{g}} \quad (7)$$

f being the frequency of the excitation.

The dimensionless problem is governed by: all the geometrical data scaled by D , the Reynolds number, and the arbitrary parameters of the excitation A and f . Notice that the dimensionless fluid constants are the density (1) and the viscosity ($1/\text{Re}$), and the field equations, equations (4), only depend on the Reynolds number; while the excitation, equation (6), is determined only by the amplitude and the excitation frequency.

In order to complete the definitions, the convective velocity, i.e., \mathbf{c} , must be determined. This velocity is, in fact, related to the mesh rezoning algorithm. It is defined as

$$c_i = \hat{v}_i - v_i \quad (8)$$

If the domain boundaries are known at every instant, \hat{v} can be prescribed accordingly. That is, the mesh motion can be described by simple ad-hoc formulas or by solving potential equations that maintain element regularity. If the boundary motion is unknown, that is the case for free surface flows, an extra equation must be solved. This equation is nothing else than the kinematic free surface condition which is a formalization of the physical condition: no particles can cross a material surface (in this case the free surface); more detailed information can be found in Huerta and Liu (1988). The other necessary condition along the free surface (the dynamic condition) states, in this case, that the free surface is a stress free boundary and, as usual, stress conditions on the boundaries are "natural boundary conditions." Therefore, it is automatically included in the weak, or variational form of equations

(4). In this case a mixed remeshing formulation is employed. The kinematic free surface boundary condition is solved along that boundary, while in the interior, the element motion is prescribed as an explicit function of the free surface vertical displacements. This reduces considerably the numerical burden of free surface computations, because remeshing takes place in the domain but the extra equation is only solved along the free surface (smaller than the complete fluid domain).

Numerical Tests

Model Definition. The goal here is to demonstrate the applicability of the ALE formulation. To illustrate the finite element code, the problem studied experimentally by Muto et al. (1985) is reproduced numerically.

The geometry is given in Fig. 1. The density of the fluid is equal to that of water $\rho = 10^3 \text{Kg/m}^3$, while the values of

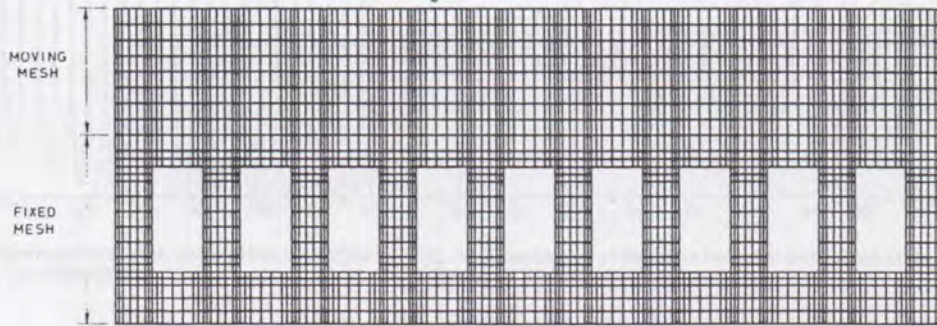


Fig. 2 Mesh discretization

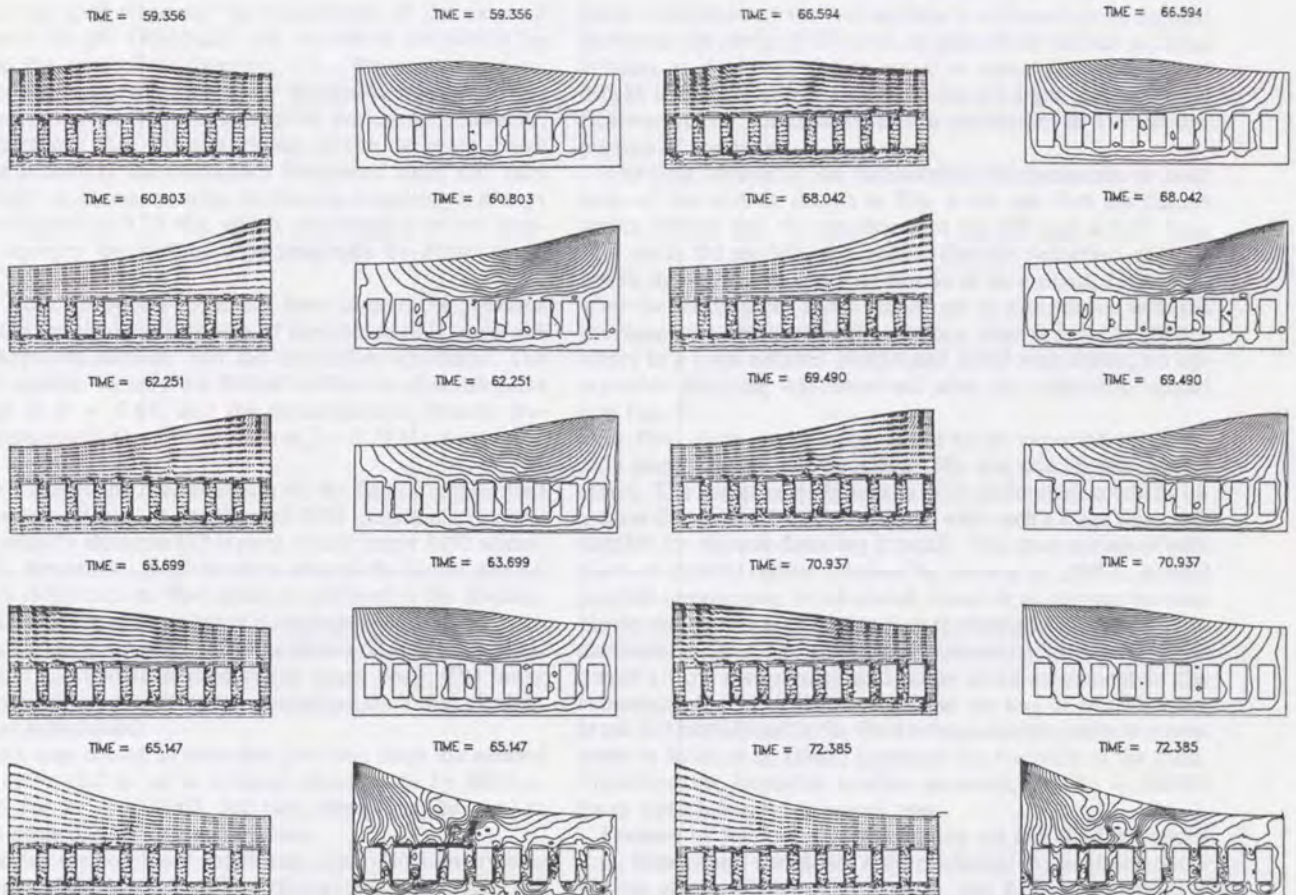


Fig. 3(a) Instantaneous configurations of the domain velocities, and streamlines for the ninth cycle

Fig. 3(b) Instantaneous configurations of the domain velocities, and streamlines for tenth cycle

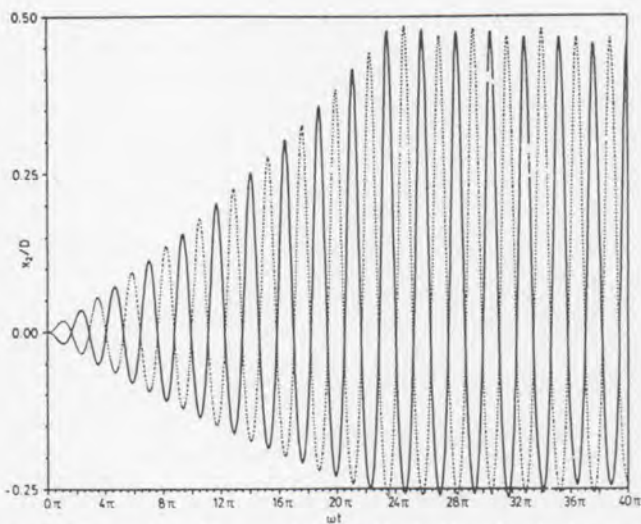


Fig. 4 Time history of the wave heights at both sides of the tank cycles and with submerged blocks, $Re = 500000$

viscosity range from $\mu = 10^{-3} \text{ Pa}\cdot\text{s}$ for water to $1 \text{ Pa}\cdot\text{s}$, because the fluid constants are not specified on the cited paper and this study intends to assess the influence of the material viscosity on the pool response. The amplitude of the external excitation is 10 gal. Obviously, the resonance frequency depends on the prescribed damping, i.e., Reynolds number. Therefore, it seems that for every Reynolds number under study the resonance frequency must be evaluated. However, it is well known that for low values of the damping (large Reynolds numbers) the resonance frequency does not vary significantly, and consequently, the forcing frequency is always prescribed equal to 0.79 Hz, which corresponds to the resonance frequency determined experimentally by Muto et al. (1985).

Apart from the geometry, it has been seen in the previous section that the sloshing response of the pool is only governed by the Reynolds number and the excitation constants. The Reynolds number varies from 500000 to 500, the dimensionless amplitude is $A = 0.01$, and the dimensionless circular frequency is obtained after substitution of $f = 0.79 \text{ Hz}$ in equation (7).

Figure 2 shows the discretization of the fluid domain used for the computations. It consists of 2758 constant pressure-bilinear velocity elements (25 layers) which imply 3052 nodes. Notice the concentration of elements around the blocks needed to capture recirculation. Two areas are defined in the domain, see Fig. 2; an Eulerian description is implemented in the bottom one (i.e., the mesh is fixed), while the mixed ALE formulation, Huerta and Liu (1988), is used in the upper zone. The latter formulation allows a continuous remeshing such that element shapes are maintained.

The time step chosen is such that 200 time steps are needed in every cycle; that is, Δt is obtained dividing 2π by $200 \times \omega$. However, for $Re = 500000$, 300 time steps must be used in the tenth cycle due to large convection.

Concerning the boundary conditions, zero velocities are prescribed around the blocks, while perfect sliding boundaries are assumed for the bottom and sides of the tank. The material surface conditions described in the previous section are imposed on the free surface.

Numerical Results. The case corresponding to pure water, i.e., $Re = 500000$, is studied first. Instantaneous configurations of the domain with velocity vectors and streamlines are plotted in Fig. 3 for the ninth and tenth cycles. At $\omega t = n\pi$ (n integer), i.e., at maximum amplitude and minimum velocity, the recirculation around the blocks is obvious. At minimum

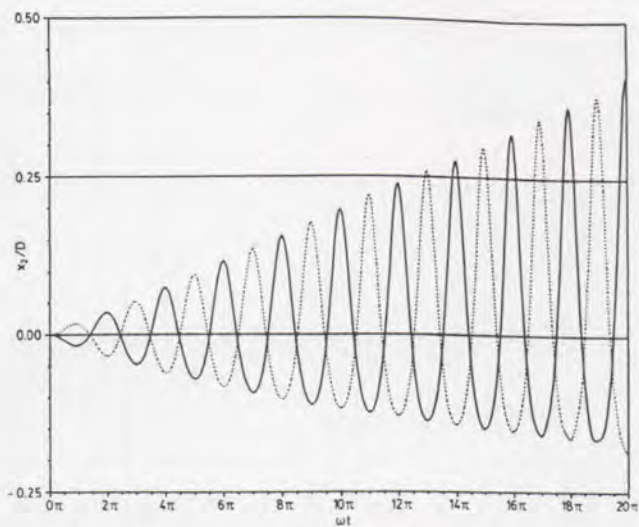


Fig. 5 Time history of the wave height at both sides of the tank without submerged blocks, $Re = 500000$

amplitude and maximum velocity, most of the flow is concentrated in the upper half of the tank; nevertheless, the flow perturbation due to the presence of blocks is clear. The non-linear evaluation of the free surface is reflected by its vertical motion at the center of the tank, in spite of the vertical material velocity at that point being equal to zero. The presence of blocks induces a reduction in the wave height and a magnification of the horizontal particle oscillation at the central portion of the tank.

The time history of the free surface displacements at both ends of the pool is shown in Fig. 4 for the first ten forced cycles. Notice that the amplitude at the left end is 0.41 (i.e., 12.4 cm in the model); this implies that the reduction of wave height due to the presence of blocks is very small, 15 percent after the tenth cycle. These results are in accordance with the previous ones obtained by the authors, Huerta and Liu (1988), where in a pool without blocks and filled with water, no appreciable damping was observed after the excitation ceased (see Fig. 5).

In fact, these conclusions ought to be expected since the only energy losses, see equations (4), are due to the viscous effect. The presence of blocks creates recirculation which increases the viscous losses; however, with such a large Reynolds number the viscous damping is small. This does not agree with the experimental results obtained by Muto et al. (1985). Several possible reasons may be advanced. Apart from the gap between blocks and glass which contradicts the hypothesis of pure two-dimensional flow, and the springs subjecting the blocks which create a flow disturbance and allow some movement of the submerged blocks; it is believed, that the loci of confetti like brass-foil introduced in the fluid to visualize the particle movement by Muto et al. (1985) increased the viscosity of the fluid. Therefore, the Reynolds number assumed, i.e., $Re = 500000$ (pure water), is not the actual one.

Because of the lack of information on the fluid constants (i.e., density and viscosity), a simple sensitivity analysis on the viscous effects is presented; that is, the Reynolds number is prescribed equal to 500 and 5000. Figure 6 shows the time history of the amplitude at the left end for all the Reynolds numbers. To be consistent with the previous analysis, during the first ten cycles forced vibrations are imposed, while free vibrations are allowed after the tenth cycle for ten more cycles.

The influence of the viscous effects is clearly observed; for $Re = 500$, a "2 π steady state" is readily obtained after the first five cycles, and the maximum amplitude is 0.09 (i.e., 2.7 cm); this is a reduction of the 80 percent compared to the case of $Re = 500000$. Moreover, the vibrations are clearly damped

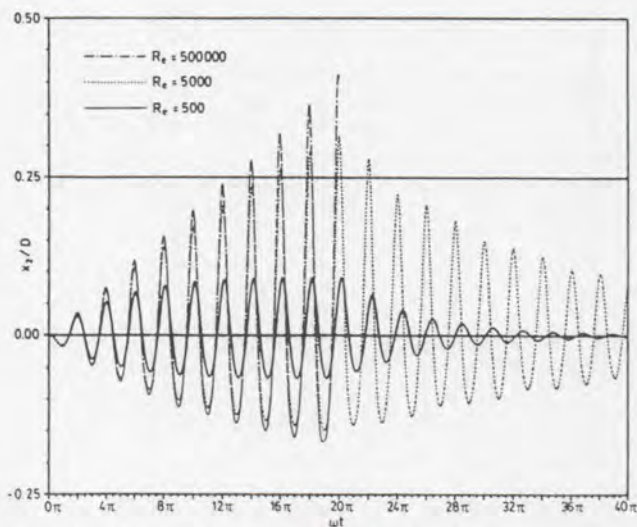


Fig. 6 Time history of the wave height at the left wall with submerged blocks

during the free vibration cycles, the measured damping factor is 6 percent.

For $Re = 5000$ no stationary maximum wave amplitude is observed after ten forced cycles. The measured value after the tenth cycle is 0.32 (i.e., 9.6 cm) which is already larger than the stationary value observed by Muto et al. (1985), i.e., 6 cm; compared to the results for pure water the reduction is however of 29 percent. Logically, the damping factor obtained for $Re = 5000$, 2 percent, is lower than the experimental one, 3 percent.

Figure 6 also shows clearly the effect of the viscosity on the resonance frequency. Notice the out-of-phase motion of the surface for $Re = 500$, while no phase lag relative to $Re = 500000$ is appreciable for $Re = 5000$ vibrating at the resonance frequency. This shows that for low damping the resonance frequency does not vary considerably and validates the choice of a constant excitation frequency.

Conclusions

Based on the results described in this study of large amplitude sloshing with submerged blocks, the following conclusions can be advanced:

- 1 The pressure-velocity mixed formulation and the streamline upwind Petrov-Galerkin techniques are now frequently used methods to compute confined incompressible flows with large Reynolds numbers and strong convective effects. The implementation of the arbitrary Lagrangian-Eulerian formulation into such preexisting codes is simple. And moreover, this formulation allows an efficient and accurate description of large free surface motions.

- 2 While resonance frequencies are easily obtained by linear codes in sloshing problems, the surface displacements depend strongly on the nonlinearities if large motions occur. The ALE description takes into account the nonlinear effects on both the surface and the interior of the domain.

- 3 Numerical tests such as the one presented herein reduce considerably the experimental costs and allow, if needed, a complete sensitivity analysis on the material properties or geometry of the problem. That is, numerical simulations which were confined to "qualitative" results, can now be used to obtain "quantitative" results.

- 4 While in the experimental analysis, the reduction of wave height is only attributed to the presence of blocks. The present analysis shows clearly the combined effect of the submerged blocks and the viscosity of the fluid. The presence of blocks

reduces in 15 percent the wave height after ten cycles when $Re = 500000$. If $Re = 5000$ the reduction in wave height is 34 percent, and if $Re = 500$ it is over 80 percent. It seems obvious, after this numerical simulation, that the presence of submerged blocks amplifies the viscous losses because of the recirculation they induce. In the experimental analysis, the loci confetti-like brass-foil introduced in the fluid to observe the particle motion may have increased the viscosity and consequently reduced the wave height. From a practical point of view, this may imply that, if the viscosity is small (large Reynolds number), the presence of blocks alone may not reduce enough the wave height to preclude a potential seismic hazard in spent fuel storage tanks.

Acknowledgments

The work of Antonio Huerta was supported by the Catalan Government under grants CIRIT AR87 and CIRIT EE88/1. The support of W. K. Liu by the National Science Foundation is also gratefully acknowledged.

References

- Belytschko, T., Kennedy, J. M., and Schoeberle, D. F., 1980, "Quasi-Eulerian Finite Element Formulation for Fluid Structure Interaction," *ASME JOURNAL OF PRESSURE VESSEL TECHNOLOGY*, Vol. 102, pp. 62-69.
- Brooks, A. N., and Hughes, T. J. R., 1982, "Streamline Upwind/Petrov-Galerkin Formulations for Convection Dominated Flows with Particular Emphasis on the Incompressible Navier-Stokes Equations," *Computer Methods in Applied Mechanics and Engineering*, Vol. 32, pp. 199-259.
- Donea, J., 1983, "Arbitrary Lagrangian-Eulerian Finite Element Methods," *Computational Methods for Transient Analysis*, eds., T. Belytschko and T. J. R. Hughes, Elsevier Science Publishers, pp. 473-516.
- Huerta, A., and Liu, W. K., 1988, "Viscous Flow with Large Free Surface Motion," *Computer Methods in Applied Mechanics and Engineering*, Vol. 69, pp. 277-324.
- Liu, W. K., Chang, H., Chen, J. S., and Belytschko, T., 1988, "Arbitrary Lagrangian Eulerian Petrov-Galerkin Finite Elements for Nonlinear Continua," *Computer Methods in Applied Mechanics and Engineering*, Vol. 68, pp. 259-310.
- Liu, W. K., and Ma, D., 1982, "Computer Implementation Aspects for Fluid Structure Interaction Problems," *Computer Methods in Applied Mechanics and Engineering*, Vol. 31, pp. 129-148.
- Muto, K., Kasai, Y., Nakahara, M., and Ishida, Y., 1985, "Experimental Tests on Sloshing Response of a Water Pool with Submerged Blocks," *Proceedings of the 1985 Pressure Vessels and Piping Conference*, Vol. 98-7 (Fluid-Structure and Dynamics), ed., S. J. Brown, ASME, pp. 209-214.
- Noh, W. F., 1964, "CEL: A Time-Dependent Two-Space-Dimensional Coupled Eulerian-Lagrangian Code," *Methods in Computational Physics*, Vol. 3, eds., by B. Alder, S. Fernbach and M. Rotenberg, Academic Press, New York.
- Pracht, W. E., 1975, "Calculating Three-Dimensional Fluid Flows at all Flow Speeds With an Eulerian-Lagrangian Computing Mesh," *Journal of Computational Physics*, Vol. 17, pp. 132-159.